Journal of Materials Processing Technology 160 (2005) 183–187

Journal of Materials Processing Technology

www.elsevier.com/locate/jmatprotec

Influence of SiC and FeSi addition on the characteristics of gray cast iron melts poured at different temperatures

K. Edalati, F. Akhlaghi*, M. Nili-Ahmadabadi

Department of Metallurgy and Materials Engineering, Faculty of Engineering, University of Tehran, P.O. Box 1136-4563, Tehran, Iran

Received 11 December 2002; received in revised form 9 June 2004; accepted 10 June 2004

Abstract

The influence of silicon carbide and ferrosilicon as silicon carriers on the cooling curve characteristics, fluidity, microstructure, chill depth and hardness of hypoeutectic gray cast irons poured at different temperatures has been investigated. It has been found that the addition of SiC instead of FeSi as a silicon carrier resulted in variations in the thermal analysis characteristics and microstructure together with increasing fluidity as well as decreasing chill depth for the whole range of pouring temperatures explored. Microstructural studies revealed that SiC addition resulted in the maximum amount of A-typed graphite with a more uniform distribution. The finest microstructure (i.e. refined eutectic cells) was also obtained with SiC addition. These observations were attributed to the pre-inoculation behavior of SiC in gray cast iron with a slow fading tendency within the melt during solidification.

Keywords: Silicon carbide; Silicon carriers; Gray iron; Cooling curve; Pouring temperature

1. Introduction

Silicon carbide is a compound containing 70% silicon (all compositions are weight percentages unless otherwise indicated) and 30% carbon. It is commercially produced by the reduction of silica sand with carbon, in the form of petroleum coke, in cylindrical electric resistance furnaces. The outer layer of the furnace product, containing approximately 90% SiC is known as metallurgical silicon carbide and can be used as an alloying additive for introducing silicon and carbon into gray cast iron [1–4], ductile iron [5–7] and steel [8] melts. Several researchers have reported the beneficial effects of SiC addition to gray cast iron melts. These include the slow fading of its inoculation effect [9], its effectiveness in improving the microstructure (especially, graphite type and distribution) [1,10], enhancing machinability [4,11] and improving mechanical properties [4]. It has also been reported [12,13] that the ability of SiC for reduction of FeO and MnO in the slag leads to increased refractory lifetime.

It has been claimed [1,4,10,11] that addition of SiC to gray cast iron (as compared with FeSi) can increase the liquidus and eutectic temperatures as well as the A-type graphite content and eutectic cell count. However, to the best of the authors' knowledge, there has been no systematic investigation of the influence of FeSi and SiC addition on the characteristics of gray cast irons poured at different temperatures. In the present study, the effects of SiC and FeSi as silicon carriers on the cooling curve characteristics, fluidity and microstructure of gray cast irons poured at different temperatures, has been quantified and compared to each other.

2. Experimental procedure

The experimental alloys were made with a constant mix of 50% cast iron scrap and 50% steel scrap of chemical compositions given in Table 1. Melting was performed using a 2.7 kHz coreless induction furnace with a nominal holding capacity of 25 kg iron. The first heat series was treated during heating with addition of FeSi (75% Si, 1.5% Al, 1% Ca, balance Fe) and the second series by addition of 90% grade

* Corresponding author.
E-mail address: fakhlagh@ut.ac.ir (F. Akhlaghi).

0924-0136/$ – see front matter © 2004 Elsevier B.V. All rights reserved.
doi:10.1016/j.jmatprotec.2004.06.007

Table 1
Chemical composition of iron and steel scraps

Materials (scrap)	C (%)	Si (%)	S (%)	P (%)	Mn (%)
Iron	3.7	2.6	0.006	0.018	0.15
Steel	0.4	0.3	0.023	0.020	0.74

granular silicon carbide (63% Si, 27% combined C, 2.5% free C, 0.03% S, remainder Al_2O_3 and SiO_2). For both series, the final chemical composition as well as the carbon equivalent (CE) of the melts was kept relatively constant by adding carbon in the form of petroleum coke (94% C, 0.35% S, 0.06% N, 0.04% H, balance ash) together with other alloying additives. The final chemical compositions of the melts are shown in Table 2. The addition of SiC, petroleum coke and 50% of the FeSi was done progressively during the melting stage and the remaining 50% of FeSi was added to the melt in the furnace (after removing the slag), 10 min before pouring into the preheated ladle at 1350 °C. The melt was poured at different temperatures (ranging from 1350 to 1500 °C) into the moulds after addition of 0.3% FeSi (of composition given above) to the melt in the ladle.

A personal computer equipped with A/D converter and K type thermocouples was used to record the cooling curves of cast iron melts poured into cylindrical CO_2–sand moulds 40 mm in diameter and 65 mm in height. Cooling curves and their first derivative curves were used to determine the undercooling of each melt (to an accuracy of ±2 °C). The spiral method was used to measure the fluidity of the melts.

The eutectic cell count was quantified by the line intercept method (accuracy, ±5%). The fraction of various graphite types was estimated visually by the point counting method (accuracy, ±5%). Cylindrical test bars (20 mm in diameter and 120 mm in height) were sectioned 20 mm from the bottom and used for metallographic examination as well as hardness measurements.

A Brinell hardness tester was used and the average value of at least five measurements was considered. W_2 chill wedge samples were used to measure chill depth (accuracy, ±0.2 mm) according to the ASTM A367-90 standard method.

Table 3
The variation of liquidus and eutectic temperatures as well as undercooling for samples treated with SiC and FeSi

Additive	Pouring temperature (°C)	Liquidus temperature (°C)	Eutectic temperature (°C)	Undercooling (°C)
SiC	1350	1188	1154	4
SiC	1400	1190	1152	6
SiC	1450	1192	1150	8
SiC	1500	1192	1145	13
FeSi	1350	1180	1144	14
FeSi	1400	1181	1144	14
FeSi	1450	1185	1140	18
FeSi	1500	1189	1132	26

3. Results

The effect of SiC and FeSi addition on the cooling curve characteristics of cast irons poured at different temperatures is summarised in Table 3. It can be seen that for both cast irons, the liquidus temperature increases, the eutectic transformation occurs at lower temperatures and the eutectic undercooling increases with increasing the melt pouring temperature. These results also show that using SiC instead of FeSi as silicon carrier increases the liquidus and eutectic temperatures and decreases the eutectic undercooling.

The variation with pouring temperature of A-type graphite percentage and eutectic cell count is shown in Fig. 1. It can be observed that for both the SiC and FeSi treated cast irons, the increased melt pouring temperature decreases the A-typed graphite content as well as the eutectic cell count. Fig. 1a shows that more A-type graphite is formed in the SiC treated melt (as compared with FeSi) and at a relatively low pouring temperature (1350–1400 °C), the SiC treated iron exhibited 100 vol.% of A-type graphite flakes. Fig. 1b shows that within the present set of experimental conditions, the eutectic cell count is higher for SiC treated irons. The typical photomicrographs in Fig. 2 illustrate the variation of graphite type and distribution in cast irons treated with SiC and FeSi, and poured at 1400 °C. These micrographs support the data presented in the Fig. 1 regarding the graphite type and also reveal the more uniform distribution of graphite flakes in the SiC treated cast irons. The variation of fluidity, chill depth and

Table 2
The additives, pouring temperatures and final chemical composition of samples (wt.%)

Additive	Pouring temperature (°C)	C	Si	Mn	P	S	Cr	Cu	CE
SiC	1350	3.40	2.11	0.912	0.021	0.052	0.359	0.605	4.111
SiC	1400	3.40	2.10	0.914	0.021	0.047	0.360	0.581	4.107
SiC	1450	3.38	2.09	0.911	0.020	0.048	0.352	0.603	4.087
SiC	1500	3.38	2.11	0.905	0.022	0.052	0.350	0.602	4.091
FeSi	1350	3.42	2.10	0.905	0.023	0.061	0.342	0.599	4.127
FeSi	1400	3.41	2.10	0.915	0.023	0.059	0.358	0.598	4.117
FeSi	1450	3.37	2.11	0.900	0.021	0.052	0.335	0.596	4.081
FeSi	1500	3.34	2.13	0.885	0.022	0.058	0.340	0.608	4.057

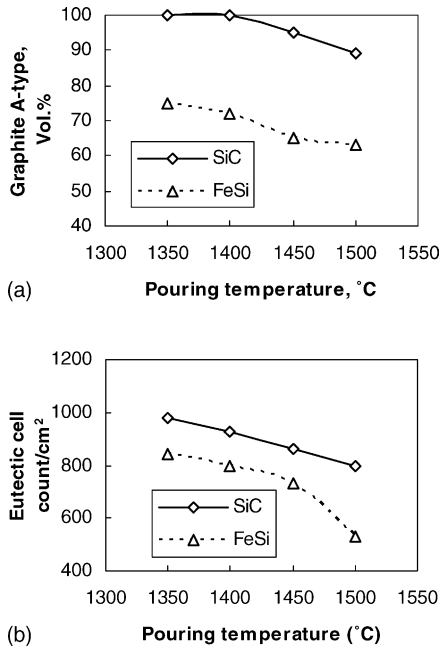

Fig. 1. The influence of SiC and FeSi addition on: (a) A-type graphite volume percentage and (b) eutectic cell count of gray cast iron melts poured at different temperatures.

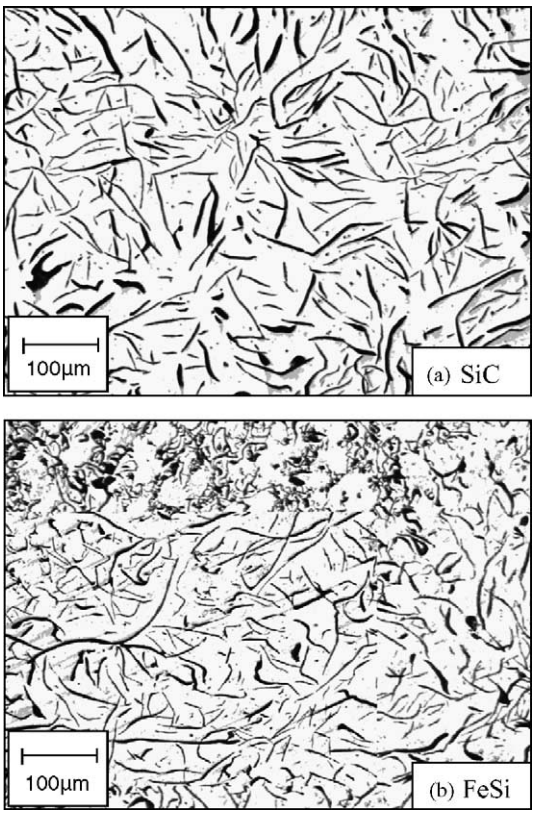

Fig. 2. Microstructure of gray cast irons containing (a) SiC and (b)FeSi, both poured at 1400 °C.

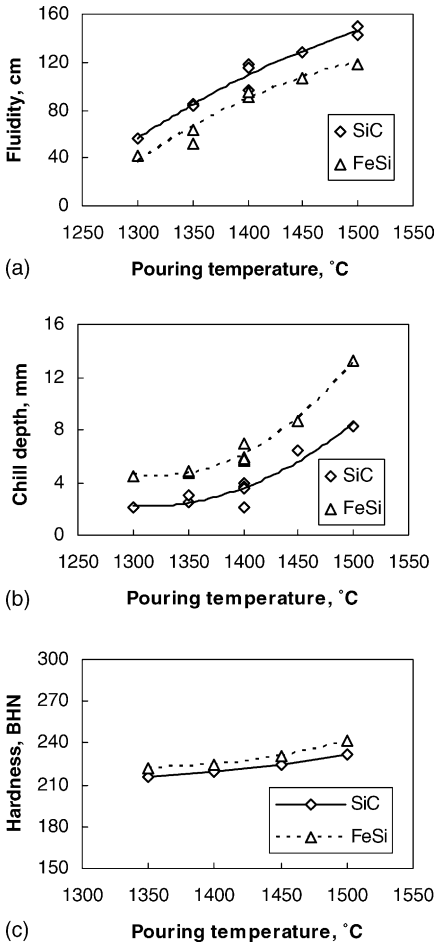

Fig. 3. The influence of SiC and FeSi addition on the (a) fluidity; (b) chill depth and (c) hardness of gray cast iron melts poured at different temperatures.

hardness with melt pouring temperature is shown in Fig. 3. It can be observed that for both the SiC and FeSi treated cast irons, the increased melt pouring temperature increases both the fluidity and chill depth and slightly increases the hardness of cast irons, while SiC treated cast irons exhibit higher fluidity as well as lower chill depth and hardness than FeSi treated ones, for the whole range of pouring temperatures explored.

4. Discussion

Numerous attempts have been made to investigate the nucleation and growth behaviour during solidification and subsequent solid-state phase transformation of cast irons by employing several techniques such as thermal analysis [14–16], metallographic techniques [17] and using physical modeling [18,19]. However, there is a general agreement to consider that austenite and graphite grow cooperatively being both in contact with liquid phase. In addition, it is well known that increasing the superheating (i) destroys the effective nuclei in the cast iron melt as a consequence of the fading of the inoculation potency and (ii) increases the un-

dercooling [20]. Consequently, the critical nuclei size radius (r^*) decreases. Therefore, the observed decrease in the eutectic temperature with increased melt superheat (Table 3) can be attributed to the decreased effectiveness of the nuclei in the cast iron. The increased eutectic undercooling for increased melt superheat, observed in the present experimental results (Table 3), has also been confirmed by other investigators [21]. This effect in turn, can explain the decreased A-type graphite content as well as the reduced eutectic cell count observed for the increased melt pouring temperature (Fig. 1), which is in agreement with other reports [21,22]. However, it has been reported [20] that the reduced critical nuclei size (r^*) is more influential in increasing the liquidus temperature. In fact, the increased superheat decreases the solidification rate via its effects on heating the mould material and consequently decreases the undercooling for austenite formation [14,21,22], therefore, the austenite formation occurs at higher temperatures (Table 3). The increased melt fluidity with increased pouring temperature (Fig. 3c) is obvious [23]. In addition, the increased chill depth observed for cast irons poured at higher temperatures (Fig. 3b) can be attributed to the decreased graphitisation tendency in the melts during solidification due to the minor decrease in the carbon equivalent for increased melt pouring temperature (Table 2), resulting in a higher carbide formation. The hardness of cast iron is influenced mainly by chemical composition and microstructural features including graphite type, graphite content and cell count. Seah et al. [22] have demonstrated that the decreased eutectic cell count with increased melt pouring temperature is accompanied with increased perlite content. Therefore, the slight increase in the hardness with increased pouring temperature can in part be attributed to the increased perlite content as a consequence of decreased eutectic cell count (Fig. 1b). Similar effects of melt pouring temperature on the cooling curve characteristics and microstructural features of gray cast iron have been reported by several authors who found increasing liquidus and solidus temperatures [24], decreased A-type graphite [25], decreased eutectic cell count [24,26] and increased chill depth [25,26].

SiC does not dissolve immediately when added to the melt and its dissolution is slow, giving a pre-inoculation effect that fades slowly and remains effective for several hours [2,9]. The pre-inoculation behavior of SiC in gray cast iron melts is not well understood, but it has been claimed [1] that during the dissolution of SiC in the melt, graphite clusters are formed around the SiC particles, as a result of local supersaturation of the melt with Si and C. These graphite clusters, which are thermodynamically metastable for a certain period of time, play an important role in the pre-inoculation effect of SiC in the melt and promote the graphite formation and eutectic nucleation. The dissolution of FeSi can also lead to graphite cluster formation, but because of its faster dissolution rate, these clusters remain stable for only short periods. Hence, during the dissolution of SiC, more graphite clusters are formed which persist for longer than during dissolution of FeSi. Formation of many graphite clusters around the SiC particles reduces the carbon content of the rest of the melt and thus nucleation of austenite occurs at higher temperatures.

In agreement with this model, SiC addition results in higher liquidus and eutectic temperatures as well as lower undercooling (Table 3), higher eutectic cell count (Fig. 1b), and lower chill depth (Fig. 3b) than FeSi for cast irons with identical melt pouring temperatures. The relatively short, randomly distributed dendrites that can form with SiC additions [1] could result in the higher A-type graphite formation observed in the SiC treated irons as shown in Fig. 1a. The higher fluidity of SiC treated cast iron melts than FeSi at identical pouring temperature (Fig. 3a) can be attributed to the increased A-type graphite as well as decreased amount of dissolved gases and inclusions [2]. These results are consistent with the reports of investigators who observed increasing liquidus and eutectic temperatures [1], increasing A-type graphite [1,2,4], increasing eutectic cell count [4,27] and decreasing chill depth [10,28] when FeSi was replaced by SiC as a silicon carrier.

5. Conclusions

The effects of addition of SiC and FeSi as silicon carriers on the fluidity, cooling curve characteristics, microstructure, hardness and chill depth of gray cast irons poured at different temperatures were investigated and the following conclusions were made:

1. The increased melt pouring temperature resulted in increased liquidus and eutectic undercooling as well as the decreased eutectic temperature. In addition, the increased melt superheating caused the decreased A-type graphite content, increased chill depth as well as decreased eutectic cell count.
2. Use of SiC addition as a silicon carrier resulted in higher liquidus and eutectic temperatures, A-type graphite content and increased eutectic cell count as well as a more uniform distribution of A-type graphite than FeSi addition.
3. Addition of SiC instead of FeSi resulted in increased fluidity and hardness together with decreased chill depth of gray cast irons.

Acknowledgment

The authors gratefully acknowledge the extension of opportunity and facilities essential for completion of this project afford to them by Iranian Casting Inc. (ICI).

References

[1] T. Benecke, A.T. Ta, G. Kahr, W.D. Schubert, B. Lux, Dissolution behavior and pre-inoculation effect of SiC in gray cast iron, Giesserei 74 (10) (1987) 301–306.

[2] T. Benecke, Metallurgical silicon carbide in electric furnace and copula furnace, Giesserei 68 (12) (1981) 344–349.
[3] I. Riposan, M. Chisamera, Use of silicon carbide in cast iron, Kohassz 126 (9) (1993) 328–330.
[4] R.L. Doelman, A.A. Beilke, A.E. Spaulding, W.J. Lau, The beneficiation of inoculated cast iron with silicon carbide as a major source of silicon and carbon, AFS Trans. 88 (1980) 787–804.
[5] T. Benecke, S. Venkateswaran, W.D. Schubert, B. Lux, The investigation of the influence of silicon carbide in production of ductile cast iron, Foundryman 87 (10) (1994) 355–360.
[6] T. Benecke, S. Venkateswaran, W.D. Schubert, B. Lux, study of the effect of silicon carbide in the manufacture of cast iron with spherical graphitr, Giesserei 80 (19) (1994) 355–360.
[7] B.C. Godsell, Pre-conditioning of ductile iron, AFS Trans. 86 (1978) 273–276.
[8] H. Heck, Silicon carbide: a review of steelmaking applications and results, in: Proceedings of the AFS International Conference on Steel Refining, Rosemont, Illinois, USA, June 2000, pp. 437–452.
[9] K.W. Caspers, Use of silicon carbide in main-frequency induction furnace, Giesserei 59 (18) (1972) 656–659.
[10] N. Kayama, N. Nakae, Y. Toyoda, Effect of silicon carbide addition on the quality and castability of cast iron, Imono 42 (3) (1970) 186–194.
[11] F. Hayama, N. Kayama, Y. Toyoda, Effect of silicon carbide addition on the machinability of cast iron, Imono 42 (3) (1970) 195–199.
[12] K.W. Copi, The use of silicon carbide in today's iron foundry, in: Proceedings of the 51st Electric Furnace Conference, Washington, DC, USA, 1993, pp. 35–38.
[13] B. Cave, Reduction of FeO in furnace slag, in: Proceedings of the 57th Electric Furnace Conference, Pittsburgh, USA, 1999, pp. 46–50.
[14] M.J. Oliveira, L.F. Malheiros, C.A. Silva Ribeiro, Evaluation of the heat of solidification of cast irons from continuous cooling curves, J. Mater. Process. Technol. 92–93 (1999) 25–30.
[15] G.L. Rivera, R.E. Boeri, J.A. Sikora, Solidification of gray cast iron, Scripta Mater. 50 (2004) 331–335.
[16] T. Mizoguchi, J.H. Perepezko, Nucleation behavior during solidification of cast iron at high undercooling, Mater. Sci. Eng. A 226–228 (1997) 813–817.
[17] N. Llorca-Isern, J. Tartera, M. Espanol, M. Marsal, G. Bertran, S. Castel, Internal features of graphite in cast irons, confocal microscopy: useful tool for graphite growth imaging, Micron 33 (2002) 357–364.
[18] G. Lesoult, M. Castro, J. Lacaze, Solidification of spheroidal graphite cast irons. I. Physical modeling, Acta Mater. 46 (3) (1998) 983–995.
[19] J. Li, L. Lu, M.O. Lai, Quantitative analysis of the irregularity of graphite nodules in cast iron, Mater. Characterization 45 (2000) 83–88.
[20] Metals Handbook, vol. 1, ninth ed., ASM, 1978, p. 170.
[21] R.W. Heine, C.R. Loper, P.C. Rosenthal, Principles of Metal casting, TMH ed., McGraw-Hill, 1976.
[22] K.H.W. Seah, J. Hemanth, S.C. Sharma, K.V.S. Rao, Solidification behaviour of water-cooled and subzero chilled cast iron, J. Alloys Compd. 290 (1999) 172–180.
[23] ASM Handbook, vol. 15, ASM, 1997, p. 11.
[24] K.H. Caspers, The effect of holding time and pouring temperature on the properties of gray cast irons melted in coreless induction furnace, Giesserei 58 (4) (1971) 77–84.
[25] H.D. Merchant, Solidification of Cast Iron, first ed., Gordon and Breach Publishers, New York, 1988.
[26] W. Paterson, H. Siempmann, W. Hauptvogel, Variation in the holding of the melt at falling temperatures, Giesserei 32 (3) (1965) 141–149.
[27] T. Benecke, Process for treating cast iron melts with silicon carbide, US Patent No. 4642135, 1978.
[28] R.L. Doelman, A.E. Spaulding, A.A. Beilke, The reaction vessel process for alloying and inoculating cupola melted cast iron, AFS Trans. 88 (1980) 123–138.